

## **New Quantum Mechanics based methods for Multiscale simulations with applications to reaction mechanisms for Electrocatalysis**

William A. Goddard III

Materials and Process Simulation Center (MSC)

California Institute of Technology, Pasadena, California 91125

**Abstract.** Electrocatalysis may provide the solution to some of the most important energy and environmental problems facing society:

- converting solar energy during the day to fuel ( $H_2$ ) that can provide power at night (hydrogen fuel cells) through water splitting
- reducing the  $CO_2$  in the atmosphere to valuable chemicals (methane, ethylene, ethanol)

However significant improvements must be made in the selectivity and activity of current electrocatalysts to obtain practical solutions. A great many experiments are underway to find such solutions, but the progress is slow. We consider that quantum mechanics based multiscale simulations can dramatically accelerate the progress by identifying the reaction mechanisms involved and the using In silico methods to predict the best modifications to Improve performance.

We will discuss some of the progress in developing the methods needed and applying them to improving electrocatalysts.

**Dedication: To Robert Grasselli, pioneer in improving catalysis and catalysts through atomistic reasoning and mechanism. Inspiration for the Irsee Catalysis meetings and for my entry into the wonderful complex world of Heterogeneous catalysis**

## **Introduction**

Proton Exchange Membrane Fuel Cells (PEMFCs) provide a most promising means for addressing the global renewable energy supply and clean environment. In particular for using Solar produced Hydrogen for power at night. Currently the main impediment for large-scale PEMFCs commercialization is the sluggish oxygen reduction reactions (ORR), which dramatically increases catalyst costs. Extensive efforts are underway to develop electrocatalysts for ORR with much higher performance and lower cost. In section 2, we describe the use of full solvent QM MD to determine the reaction mechanism and the use of the ReaxFF reactive force field to explain the activity of the new dealloyed jagged nanowire catalysts.

Electrochemical CO<sub>2</sub> reduction to value-added fuels and feedstocks offers solutions to the shortage of renewable energy sources while remediating CO<sub>2</sub> emission from human activity. Copper (Cu) is effective at reducing CO<sub>2</sub> to hydrocarbons or oxygenates, but low product selectivity and short production stability impede practical applications. In section 3 we summarize the new methods of QM that are being used to make progress in realistic simulations of current catalysts and the interplay of QM, ReaxFF reactive FF, and machine learning to explain current experiments and to design new electrocatalyst.

The oxygen evolution reaction (OER) is an important reaction and often a limiting step in many electrochemical devices that hold great potential for clean energy conversion and fuel transformation, such as water electrolyzers rechargeable metal-air batteries and electrochemical synthesis. There has been extensive effort over past decade for new OER catalysts that exhibit the required activity, durability, and selectivity. But increased activity and selectivity is needed. In section 4 we summarize the progress in realistic simulations of current catalysts and the progress in explaining current experiments on new electrocatalyst.

Sections 2, 3, and 4 made extensive use of QM to determine fundamental mechanisms and rates, but we saw that the size and time scales of QM (100's of atoms, 10's of picoseconds of MD) severely restrict its use for developing next generation electrocatalysts. We must use reactive force fields to describe the chemistry and reactions of the millions to billions of atoms required even for scales on 10 – 100 nm. Section 5 outlines some of the progress and directions.

## **2. the Oxygen Reduction Reaction on Pt based fuel Cells**

The hydrogen fuel cell is very simple. The anode catalyst dissociates H<sub>2</sub> to form electrons (current or power) and protons that go through the membrane to combine with O<sub>2</sub> to form H<sub>2</sub>O at the cathode. It is this Oxygen Reduction Reaction that is far too slow (400 times slower than the anode chemistry). To understand the mechanism for ORR, we carried out reactive dynamics using forces from QM (QM MD or AIMD). Since hydrogen bonding in the solvent is important we included 5 layers of solvent (all the reactions occur in the first three layers). [1] In order to obtain accurate activation free energies at 298 K, we used meta dynamics to sample the transition state sufficiently. The QM metadynamics methodology was invented in 2002 [2] but had not previously been used for full solvent calculations because equilibrating the 5 layers of solvent might take 1 ns of MD, whereas it is not practical to do QM MD on a system with 100's of atoms for more than ~ 40 ps.,

We solved this problem by doing the 1 ns of equilibration with the ReaxFF for water [3] and then converting to QM, which equilibrates in an additional 10 ps. Because

We discovered that the mechanism is as follows [1]

1.  $\text{H}^* + \text{O}_2 \rightarrow \text{HOO}^*$
2.  $\text{H}^* + \text{HOO}^* \rightarrow \text{H}_2\text{O} + \text{O}^*$
3.  $\text{O}^* + \text{H}_2\text{O}^* \rightarrow \text{OH}^* + \text{OH}^*$
4.  $\text{OH}^* + \text{H}_3\text{O}^+ \rightarrow \text{H}_2\text{O} + \text{H}_2\text{O}$

where surface species are denoted with \*. The QM metadynamics allowed to understand the nature of step 4, which becomes rate limiting above 0.9 V. The transition state is shown in Fig. 1. It shows that 5 H<sub>2</sub>O are involve in a Grotthuss mechanism in which the proton is simultaneously transferring between all 5 H<sub>2</sub>O and OH\* at the transition state!

We found that for applied potentials  $U < 0.9$  V the rate determine step is (3), hydration of O\*,  $\text{DG}_{\text{act}} = 0.25$  eV but above 0.9 V, the barrier increases to 0.4 eV at  $U=1.23$  V. Fig. 2 shows the predicted  $\Delta\text{G}_{\text{act}}$  vs.  $U$  and compares to experiments by Nenad Marcovic of ANL.[4] We see that the predicted  $\text{DG}_{\text{act}}$  are within 0.05 V of the experiment. This is good news since this is the accuracy needed to use theory to develop improved catalysts.

A major step forward in ORR catalysts was made by Yu Huang (UCLA) and coworkers, [5] who showed in 2016 that starting with a 5 nm wire with composition Ni<sub>7</sub>Pt<sub>3</sub> and reacting away all the Ni, leads to a **jagged nanowire (NW) with 50 times higher activity than state of the art Pt/C with long lifetime**. The ReaxFF predicted structure is shown in Fig. 3. This surface has a number of undercoordinated site but there was no clear idea from the structure why the activity would increase so dramatically. [5] We have struggled to understand this for 3 years and just recently Yalu Chen made a breakthrough in discovering that the dealloyed surface leads to regions that are concave such that the binding site for H<sub>2</sub>O\* is forced to bind next to that of O\*, (see Figure 4) leading to a very low barrier for reaction (3), the rate determining step. [6] The next challenge is building such sites into practical electrodes.

### 3. Electrochemical CO<sub>2</sub> reduction to value-added fuels and feedstocks

#### 3.1 Full solvent QM

In order to determine the reaction mechanism for reducing CO<sub>2</sub> to hydrocarbons or oxygenates, we again used full solvent (5 layers) QM based metadynamics to determine the free activation barriers for each reaction step.

Here we considered CO reduction at neutral pH to compare to experiments. [7] The resulting mechanism is shown in Fig. 5. We see that there are 10 steps from CO\* to ethylene with the highest  $\Delta\text{G}_{\text{act}} = 0.69$  eV. There are also 10 steps from CO\* to ethanol, where the first six to HOCCH are in common with those to ethylene. [7,8] The preference toward ethylene over ethanol is determined by the relative barriers  $\text{DG}_{\text{act}} = 0.61$  eV vs. 0.67 eV, which would lead to 11 times more ethylene than ethanol. [7,8] The experimental ratio [8] indicates that  $\delta\Delta\text{G}_{\text{act}} = 0.066$  instead of 0.06 eV suggesting a relative accuracy of better than 0.01 eV!

These results that QM MD metadynamics at the standard PBE-D3 level of DFT can provide such accuracy is great news, allowing us to determine the fundamental reaction mechanisms and kinetics on low index surfaces of electrocatalysts.

The Feng Jiao group at Delaware discovered that adding amines into the CORR system could lead to 40% FE for production of acetamides, thus forming CN bonds not just oxygenated products. [9] We applied full solvent QM metadynamics and discovered a branch of the above mechanism in which the HOCCOH species can form a ketene-like intermediate that can react with amines to form acetamide as shown in fig. 6. [9]

### 3.2 Nanoparticles (200,000 atoms) much better, use ReaxFF reactive Force field

The bad news is that experimentally the best catalysts are nanoparticles (NP) with sizes of 10-20 nm. These NP have ~200,000 atoms and ~10,000 surface sites, well beyond the ~200 atoms per cell practical for QM MD. Thus Kanen and coworkers [10] showed that depositing 10-20 nm Cu NP on 9 nm carbon nanotubes led to FA>70% for CORR to ethanol at -0.3 V, finding that the production correlated with grain boundary density.[10]

This is clearly well beyond the realm of QM. In order to study such systems we use the ReaxFF reactive force field methodology developed by van Duin and Goddard in 2002.[11] ReaxFF treats electrostatics between ALL atoms, not just the ones that are not bonded. This is because the bonds are allowed to break and rearrange. To do this the charge on an atom is described by a Gaussian function the size of the atom. This allows the charges of bonded atoms to be shielded. In addition the charges are allowed to flow from atom to atom during the dynamics, as needed for bond rearrangements. The magnitudes of the charges are predicted using the Charge Equilibration (QEq) method, [12] which uses atomic ionization potential and electron affinity to predict charge transfer. This was established recently to accurately describe the charges from QM.

In addition the bonds are allowed to break. Here the bond order is allowed to change exponentially with distance and a bond energy bond order relationship is fitted to QM. For the oxidative dehydrogenation of propane by a  $V_4O_{10}$  cluster representing the  $V_2O_5$  catalyst this led to accuracies of 0.1 to 0.25 eV in the reaction barriers compared to QM. [13] Figure 7.

Using ReaxFF we simulated the CVD of Cu onto 9 nm CNT, leading to the result in Fig 8. [14] This structure led to simulated XRD and TEM patterns in agreement with experiment. [14] Moreover, the Temperature Programmed Desorption (TPD) experiments showed that ~15% of the CO bond to the NP much stronger than for the low index surfaces and our calculations based on our predicted NP found the same. [14]

To determine what kind of sites lead to the selective production of ethanol, we used QM to predict the CO binding to ~200 sites and selected the 4 strongest to analyze. Of these 4 we found that two had a dramatically reduced activation energy to form the transition state leading to ethanol. These sites involved a stacking fault induced by the grain boundary, (see figure 9) leading to a barrier 0.18 eV lower for ReaxFF and 0.11 eV lower for QM. [14] This is consistent with experiment, showing the power of combining ReaxFF with QM.

### 3.3 11,000 surface sites too many to do all of them; Use machine learning to predict all of them

But the bad news is that we only examine CO binding for 200 out of 11,000 surface sites and we did activation barriers only for 4 sites. How can we know we found the best ones? **We need a fast way to predict binding at all 11,000 sites. ANSWER Develop Machine Learning model.** This was developed in [15]. For each surface site we calculated the QM energy using a 8Å cutoff and inputted the interatomic distances using 2 and 3 body terms and used localized cosine piecewise basis functions. Fig 10. This was trained with the QM and used to predict new points until the



Refined Machine Learning model obtained 0.05 eV accuracy (takes 500-800 calculations).[15] Then we used the ML to predict the other 11,000 sites (very fast). [15] Fig 11 shows the predicted CO bonding energy for all 11,000 sites, and Fig. 12 shows the predicted optimum site (periodic 4x5 unit cell) predicted to yield 96% FE for CORR to ethanol. [15]

## 4. Water splitting

### 4.1 Oxygen evolution reaction (OER) on doped $\gamma$ -NiOOH

To obtain the H<sub>2</sub> for fuel cells to provide power at night, we need to use solar energy to convert water to H<sub>2</sub> and O<sub>2</sub> during the day, water splitting. IrO<sub>2</sub> has been the best for acid conditions, but it is unstable in basic conditions. Experimentally Fe doped NiOOH with the  $\gamma$ -NiOOH structure is the best with a Tafel Slope of 30 meV/dec and an over potential of ~0.37 V. We used our new Grand Canonical QM techniques to determine the mechanism; however we had to go beyond the standard PBE-D3 level, because the level does very badly in describing the triplet state of O<sub>2</sub>. [16] Using the B3PW91 hybrid DFT (with the CRYSTAL code) we predicted the kinetics shown in Figure 13 with an overpotential 0.42V and Tafel Slope=23 mV/dec compared to 0.37 V and 30 mV/dec experimental. [16] We discovered that the key to OER is that the Fe=O bond must have  $\pi^*$  radical character on the O atom in order to facilitate forming the OO bond from OH derived from H<sub>2</sub>O in the next step.

The details shown in Fig. 13 are as follows. We consider two Fe dopant atoms distributed among the 12 Ni sites, mimicking the fraction with the best performance.

- the first oxidation step converts Ni<sup>3+</sup> with an unpaired spin to Ni<sup>4+</sup> bonded to OH-derived from solvent H<sub>2</sub>O along with proton coupled electron transfer (PCET). The change in free energy is  $\Delta G=2.04$  eV
- The second oxidation converts subsurface Ni<sup>3+</sup> to Ni<sup>4+</sup> while deprotonating the OH at the surface Fe<sup>4+</sup>, leading to an unpaired spin on the Fe=O bond. The change in free energy is  $\Delta G=1.20$  eV
- The third step is coupling the O of a solvent H<sub>2</sub>O to a surface M=O bond while removing the H from the O. Doing this at the surface Fe leads to a barrier of 0.66 eV with a net  $\Delta G=0.60$  eV, but doing it at the Ni site leads to a barrier of 0.64 eV with a net  $\Delta G=-0.23$  eV. Thus both Ni<sup>4+</sup> and Fe<sup>4+</sup> play a role in the high performance.
- Subsequent oxidation steps re-oxidize Fe back to 4+ and then remove the H from HOONi and then desorb O<sub>2</sub> product.
- Using the reaction barrier free energies we calculate a current of 10mA/cm<sup>2</sup> at an overpotential of 0.42 V in reasonable agreement with the experimental value of ~0.37 V.

An interesting result from these calculations is that the (Ni,Fe)OOH catalyst is bifunctional: With both Ni and Fe providing core functionalities for driving the OER, • The surface Fe(IV) site with a high spin d 4 configuration stabilizes the key active O radical intermediate, • While the surface Ni(IV) site with its closed shell d 6 configuration takes charge of catalyzing the O–O coupling that is a key step toward the O<sub>2</sub> product. Thus, it is the synergy between Fe and Ni that delivers the optimal performance of (Ni,Fe)OOH for catalyzing the OER. A second feature for the case with two Fe dopant atoms is that the superoxide (\*O<sub>2</sub>) intermediate on Ni is stabilized by a small free energy barrier of 0.1–0.2 eV. I

These results are quite encouraging, showing that we get kinetics quite consistent with experiment. Then we built upon this result by replacing Fe with the 18 transition metals of the Ti-Co columns

but using the mechanistic result that radical character was needed on the M=O bond. [17] We found that only Co, Rh, and Ir satisfied this condition (in addition to Fe). Then using slightly more approximate methods we estimated that the Co, Rh, and Ir would have overpotentials 0.18, 0.30, and 0.43 eV lower than Fe, making it very interesting to examine Ir further. [17]

This led to a collaboration with the Jianming Wang group at Zhejiang University in Hangzhou China, who used a novel photochemical deposition method to prepare a hierarchical layered Ir-modified NiCoOOH/ZnO@NCC composite film, with 8% Ir, 46% Co, and 46% Ni. [18] They found much improved results with 20 mA/cm<sup>2</sup> at an overpotential of 0.20 V! We did QM constant potential calculations and found that 8% Ir was quite favorable. [18] In particular the theory and experiment agree that at and above the 0.20 V onset potential the Ir at the surface is mostly 5+.

[18] It is very encouraging that the GC QM calculations for OER lead to results in excellent agreement with experiment, but **the big uncertainty has been whether our assumed surface structure is in fact the same as the one in the experiments.**

#### 4.2 OER on Co doped TiO<sub>2</sub>

A recent breakthrough here is that Prof. Sen Zhang of U. Virginia has developed a synthetic procedure for TiO<sub>2</sub> with 12% Co that leads to a crystal NP in which the surfaces are all {210}. [19] Here we used our new formulation of the GC QM in which we include the effect of applied potential on the transition state. The final results are shown in Fig. 14. [19]

The results are

at  $\eta=300$  mV:

- GCQM: TOF = 13.1 s<sup>-1</sup> per surface Co site
- experiment: TOF = 9.1 s<sup>-1</sup> per surface Co site

at  $\eta=400$  mV:

- GCQM: TOF = 307.4 s<sup>-1</sup> per surface Co site;
- experiment: TOF = 249.2 s<sup>-1</sup> per surface Co site

Tafel slope: GCQM: 74 mV/dec; experiment 72 mV/dec.

**These results show spectacular agreement.** These results would be in exact agreement if in the experiment 28% of the surface sites are inactive. Also they would agree if the GCQM barrier is shifted to be 0.01 eV higher. Now we can do in silico examination of all possible dopants to predict the best possible catalyst.

#### 5.0 Multiscale Simulations

In the above sections we showed that QM calculations at the DFT level with explicit solvent or under constant potential conditions are now capable of making predictions on new materials with accuracies often good to 0.05 eV and to overpotentials often good to 0.05 V. this is very good news, because this is the level of accuracy needed for theory to play a role in discovering new high performance systems.

However we also saw that greatly improved performance is found for nanoparticles and particularly dealloyed particles. This requires spatial scales of 10's nm which very quickly leads to systems with 100,000's of atoms to millions. Such sizes are not practical for QM, but we found

that the ReaxFF reactive force can describe the structures and dynamics of these larger systems. However ReaxFF does not usually get the accuracy of 0.05 eV of QM. This is why our studies on the NP used QM calculations on clusters extracted from the NP. **Thus a major challenge now is to improve the reactive FF to achieve a 0.05 eV level of accuracy.**

We have started this development of a new reactive FF, RexPoN, that aims at retaining the 0.05 eV level of accuracy of ab initio QM, but we want it to be more accurate than DFT for bond breaking and hydrogen binding interactions. The idea is to separate out the long range interactions: van der Waals (London dispersion) attraction and electrostatics (allowing charge transfer and polarization). Then use very accurate ab initio methods (coupled cluster CCSD(T)) for hydrogen bonds and bond breaking. [25]

The elements are:

1. **PQEq Charge and Polarization model.** [21-23] Tested against QM, PQEq predicts accurately the polarization as point dipoles are brought into various molecules. (see Fig. 15) **PQEq uses Gaussian shaped charges (not point charges) on each atom plus Gaussian shell charge to Describe charge transfer & polarization**
2. Determine **non-bond parameters from PBE-D3 or B3LYP-D3 QM** that describe Equation of State for molecular solids up to 100 GPa. Extract pure Pauli Principle repulsion (PR) and pure London dispersion (LD) attraction. [24]
3. Given PR and LD, extract valence parameters to **fit exactly highest quality ab initio QM (CCSDT) for bond breaking** and reactions. Describe by ReaxFF formalism. [20]
4. Add in **Hydrogen Bonding corrections from QM on dimers at CCSDT.** 30,000 points fitted to analytic functions to  $\sim 4 \text{ cm}^{-1}$  (Joel Bowman, Emory)

Applying RexPoN to liquid water leads to the spectacular results shown in Fig. 16. [20] We will be developing RexPoN over the next couple of years.

An essential issue with such methods is that they be transferable. That is they must give comparable accuracy for systems on which they were not trained. This will be a challenge but we are hopeful.

If we can retain the 0.05 eV accuracy for a transferable FF, it will no longer be necessary to continually go back to cutting our clusters small enough for QM

## 6. Summary and Conclusions

The examples described above illustrate that It is now becoming feasible to combine QM based multiscale simulation with machine learning to discover new paradigms for materials and to drive the design and development of new catalysts and materials. This is fortunate because society needs to dramatically accelerate progress in developing practical electrocatalysts with performance sufficient to dramatically accelerate production of renewable energy to meet the needs of our rapidly expanding population. Similarly we need to develop energy efficient and selective ways to convert CO<sub>2</sub> to valuable chemicals, to generate NH<sub>3</sub> efficiently from N<sub>2</sub>, and to reduce the O<sub>2</sub> to H<sub>2</sub>O in fuel cells with efficient low cost electrocatalysts.

## Acknowledgements

The research on CO<sub>2</sub> reduction was supported as part of the Joint Center for Artificial Photosynthesis, an Energy Innovation Hub funded by the U.S. Department of Energy, Office of Science. (DE-SC0004993)

The research on ORR is funded by ONR (N00014-18-1-2155). The research on OER is funded by NSF (CBET-1805022). There is no direct funding for RexPoN, but it is supported by these other projects.

### **Conflict of Interest.**

We declare no Conflicts of Interest.

### **References**

- 1- “Mechanism and kinetics of the electrocatalytic reaction responsible for the high cost of hydrogen fuel cells.” T. Cheng; W.A. Goddard III; Q. An; H. Xiao; B. Merinov & S. Morozov. *Physical Chemistry Chemical Physics* 19 (4):2666–2673 (2017) wag1248.
- 2-A. Laio and M. Parrinello, *Proc. Natl. Acad. Sci. U.S.A.* 99, 12562 (2002).
- 3- A ReaxFF Reactive Force-field for Proton Transfer Reactions in Bulk Water and its Applications to Heterogeneous Catalysis. A.C.T. van Duin; C. Zou; K. Joshi; V. Bryantsev & W.A. Goddard. Chapter 6 in *Computational Catalysis*, A. Asthagiri and M.J. Janik, Ed. Royal Society of Chemistry, pp.223–243 (2013) wag1046.
- 4- (a) B. N. Grgur, N. M. Marković and P. N. Ross, *Can. J. Chem.*, 1997, 75, 1465–1471  
(b) U. A. Paulus, A. Wokaun, G. G. Scherer, T. J. Schmidt, V. Stamenkovic, V. Radmilovic, N. M. Markovic and P. N. Ross, *J. Phys. Chem. B*, 2002, 106, 4181–4191
5. Ultrafine jagged platinum nanowires enable ultrahigh mass activity for the oxygen reduction reaction. M. Li; Z. Zhao; T. Cheng; A. Fortunelli; C.-Y. Chen; R. Yu; Q. Zhang; L. Gu; B.V. Merinov; Z. Lin; E. Zhu; T. Yu; Q. Jia; J. Guo; L. Zhang; W.A. Goddard III; Y. Huang & X. Duan. *Science* 354 (6318):1414–1419 (2016) wag1194.
6. Explanation of the Dramatically Improved Oxygen Reduction Reaction of Jagged Platinum Nanowires, 50 times better than Pt. Yalu Chen, Tao Cheng, William A. Goddard III. *JACS* submitted
7. Full atomistic reaction mechanism with kinetics for CO reduction on Cu(100) from ab initio molecular dynamics free-energy calculations at 298 K. T. Cheng; H. Xiao & W.A. Goddard III. *Proc. Natl. Acad. Sci. U.S.A.* 114 (8):1795–1800 (2017) wag1251.
8. Electrochemical CO reduction builds solvent water into oxygenate products. Y. Lum; T. Cheng; W.A. Goddard III & J.W. Ager. *J. Am. Chem. Soc.* 140 (30):9337–9340 (2018) wag1291.
9. Formation of carbon–nitrogen bonds in carbon monoxide electrolysis. M. Jouny; J.-J. Lv; T. Cheng; B.H. Ko; J.-J. Zhu; W.A. Goddard III & F. Jiao. *Nat. Chem.* 11 846–851 (2019) wag1349.
10. A Direct Grain-Boundary-Activity Correlation for CO Electroreduction on Cu Nanoparticles; Xiaofeng Feng; Kaili Jiang; Shoushan Fan, Matthew W. Kanan; *ACS Cent. Sci.* 2016, 2, 169-174z

11. ReaxFF: A Reactive Force Field for Hydrocarbons. A.C.T. van Duin; S. Dasgupta; F. Lorient & W.A. Goddard III. *Journal of Physical Chemistry A* 105 (41):9396–9409 (2001) wag471.
12. Charge equilibration for molecular dynamics simulations. A.K. Rappe & W.A. Goddard. *J. Phys. Chem.* 95 (8):3358–3363 (1991) wag264.
13. Single-Site Vanadyl Activation, Functionalization, and Reoxidation Reaction Mechanism for Propane Oxidative Dehydrogenation on the Cubic  $V_4O_{10}$  Cluster. M.-J. Cheng; K. Chenoweth; J. Oxgaard; A. van Duin & W.A. Goddard III. *Journal of Physical Chemistry C* 111 (13):5115–5127 (2007) wag706.
14. Nature of the active sites for CO reduction on copper nanoparticles; suggestions for optimizing performance. T. Cheng; H. Xiao & W.A. Goddard III. *Journal of the American Chemical Society* 139 (34):11642–11645 (2017) wag1232.
15. Identification of the Selective Sites for Electrochemical Reduction of CO to  $C_{2+}$  Products on Copper Nanoparticles by Combining Reactive Force Fields, Density Functional Theory, and Machine Learning. Y. Huang; Y. Chen; T. Cheng; L.-W. Wang & W.A. Goddard III. *ACS Energy Letters* 3 (12):2983–2988 (2018) wag1308
16. Synergy between Fe and Ni in the optimal performance of (Ni,Fe)OOH catalysts for the oxygen evolution reaction. H. Xiao; H. Shin & W.A. Goddard III. *Proc. Natl. Acad. Sci. U.S.A.* 115 (23):5872–5877 (2018) wag1286.
17. In silico discovery of new dopants for Fe-doped Ni oxyhydroxide ( $Ni_{1-x}Fe_xOOH$ ) catalysts for oxygen evolution reaction. H. Shin; H. Xiao & W.A. Goddard III. *J. Am. Chem. Soc.* 140 (22):6745–6748 (2018) wag1284.
18. NiCoIr Oxyhydroxide Nanosheet: Highly Efficient and Stable Electrocatalysts for the Oxygen Evolution Reaction; Liang-ai Huang, Hyeyoung Shin, William A. Goddard III, and Jianming Wang; submitted
19. Oxygen Evolution Reaction over Catalytic Single-Site Co in Well-Defined Brookite  $TiO_2$  Nanorod Surface: Experiment with Quantum Mechanics Validation; Chang Liu, Jin Qian, Yifan Ye, Hua Zhou, Cheng-Jun Sun, Colton Sheehan, Zhiyong Zhang, Gang Wan, Yi-Sheng Liu, Jinghua Guo, Shuang Li, Sooyeon Hwang, T. Brent Gunnoe, William A. Goddard III, Sen Zhang; submitted
20. The quantum mechanics-based polarizable force field for water simulations. S. Naserifar & W.A. Goddard III. *J. Chem. Phys.* 149 (17):174502 (2018) wag1305.
21. Polarizable charge equilibration model for predicting accurate electrostatic interactions in molecules and solids. S. Naserifar; D.J. Brooks; W.A. Goddard III & V. Cvicek. *J. Chem. Phys.* 146 (12):Art. No. 124117 (2017) wag1213.
22. Extension of the Polarizable Charge Equilibration Model to Higher Oxidation States with Applications to Ge, As, Se, Br, Sn, Sb, Te, I, Pb, Bi, Po, and At Elements. J.J. Oppenheim; S. Naserifar & W.A. Goddard III. *Journal of Physical Chemistry A* 122 (2):639–645 (2018) wag1262.
23. The polarizable charge equilibration model for transition-metal elements. S. Kwon; S. Naserifar; H.M. Lee & W.A. Goddard III. *J. Phys. Chem. A* 122 (48):9350–9358 (2018) wag1294.

24 Accurate non-bonded potentials based on periodic quantum mechanics calculations for use in molecular simulations of materials and systems. S. Naserifar; J.J. Oppenheim; H. Yang; T. Zhou; S. Zybin; M. Rizk & W.A. Goddard III. J. Chem. Phys. 151 (15):Art. No. 154111 (2019) wag1357.

25. Accurate *ab initio* and “hybrid” potential energy surfaces, intramolecular vibrational energies, and classical ir spectrum of the water dimer; Shank, Y.Wang, A. Kaledin, B. J. Braams, and J. M. Bowman, J. Chem. Phys. 130(14), 144314 (2009).

## Figures

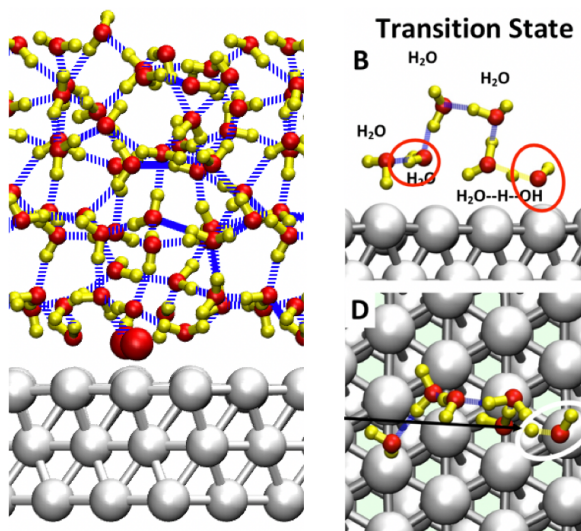


Figure 1

Left: Side view of Surface structure of water/Pt(111) interface used in the full solvent metadynamics QM simulations of ORR on Pt(111). Right: the side and top view of the transition state for the last step of ORR, protonating surface OH\* to form H<sub>2</sub>O. This involves a Grotthuss chain of 5 waters. [1]

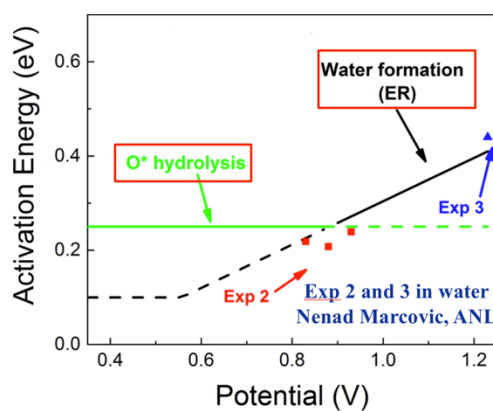
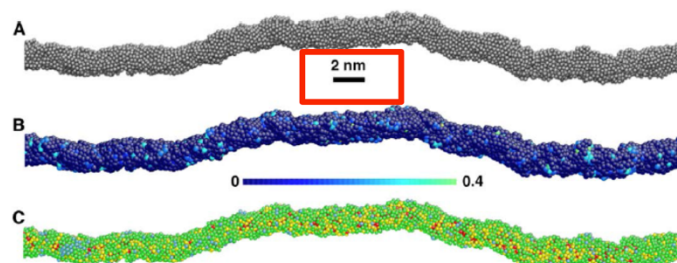


Figure 2. the activation energy at 298 K from full solvent QM metadynamics for ORR on Pt(111). Normal operating potential is 0.9 V RHE, because the rate is too slow at 1.23 V. The predicted activation barrier at 0.9 and 1.23 V are within 0.05 eV of the Nenad Marcovic experiments. This is good news because the theory needs to have this accuracy to predict improved catalysts. [1]

Figure 3. Structure predicted from ReaxFF reactive dynamics simulations for Yu Huang's jagged Pt nanowires (NW) that are 50 times faster than standard Pt/c. Just as in the experiment, we started we started with a 5 nm NW that was 70%Ni and 30% Pt and reacted away the Ni while relaxing the structure of the Pt, ending with a 2 nm jagged Pt NW. [5]





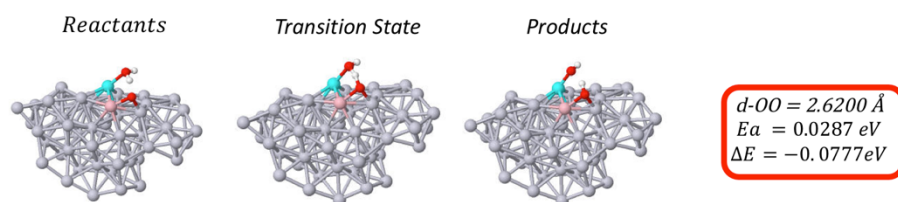
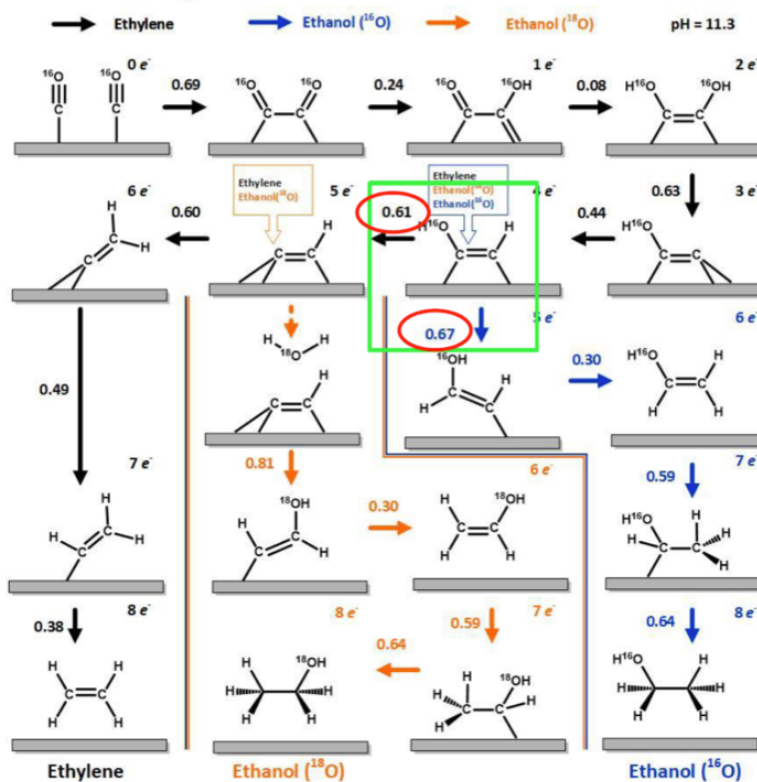


Figure 4. About 1/3 of the surface sites on the Jagged Pt NW in Figure 3 have convex sites like this in which the O\* binds to two Pt of a surface triangle while the H<sub>2</sub>O binds to the third atom, leading to a very short distance of the water OH from the surface O\* and hence a very low barrier and hence a very low energy barrier. [6]

Figure 5. Reaction mechanism for reducing CO to ethylene and ethanol from full solvent QM metadynamics. Both ethylene and ethanol require 10 steps, the first 6 of which are in common (up to the green square). The relative free energy barriers of 0.61 and 0.67 eV predict that the ratio of ethylene to ethanol should be 11. The observed ratio of 14 suggests that then energy difference is 0.066 not 0.06 indicating that the QM may be high by 0.006 eV. [7. 8]



Add NH<sub>3</sub> get C-N bonds

Mechanism for CO reduction on copper splits at [HOC=COH] into two pathways:

\*C=COH (producing ethylene, ethanol and n-propanol) and

\*C=C=O which can form acetate

**Much more interesting is that adding NH<sub>3</sub>. MeNH<sub>2</sub>, and (Me)<sub>2</sub>NH leads to acetamides**

structure of \*C=C(OH)NH<sub>2</sub>, the first reactive intermediate with an C-N bond.

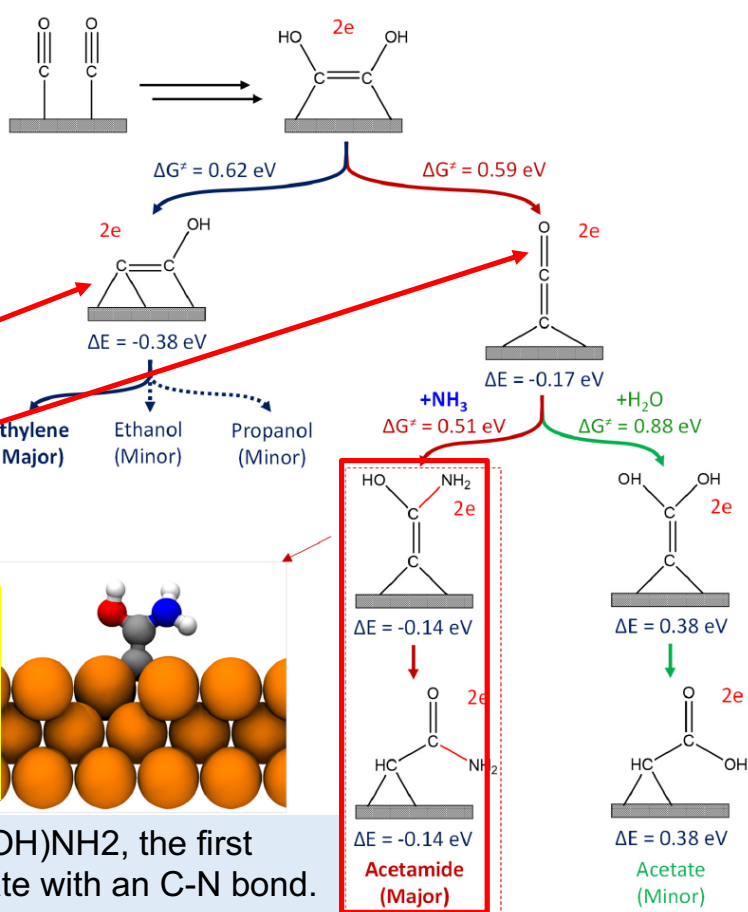


Figure 6. The extended mechanism from Figure 5, showing how the CN bond to form acetamides occurs when NH<sub>3</sub> is present. [9]

Figure 7

Comparison of the predicted energies from QM and ReaxFF for the oxidative dehydrogenation of propane to propene plus the deoxidation by O<sub>2</sub> to recover the catalyst. ReaxFF reproduces the overall mechanism quite well with energies within 5 kcal/mol or 0.2 eV.[13]

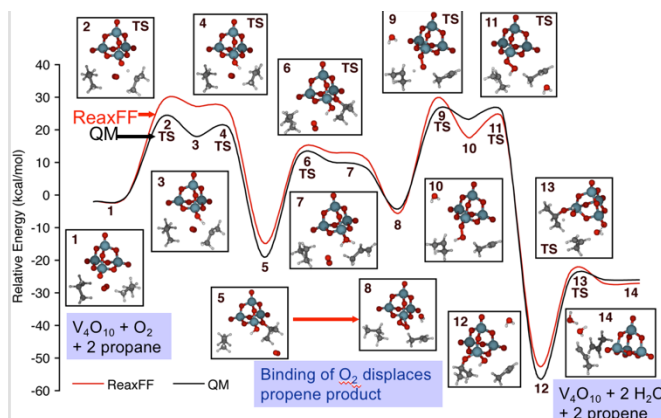


Figure 8. the Cu nanoparticle grown with ReaxFF, one atom at a time onto a 9 nm carbon nanotube. This matches the

size and shape in the Kanen experiments, The predicted XRD and TEM also match the experiment. The final NP has 201.755 atoms, with 11,000 surface atoms. [14]

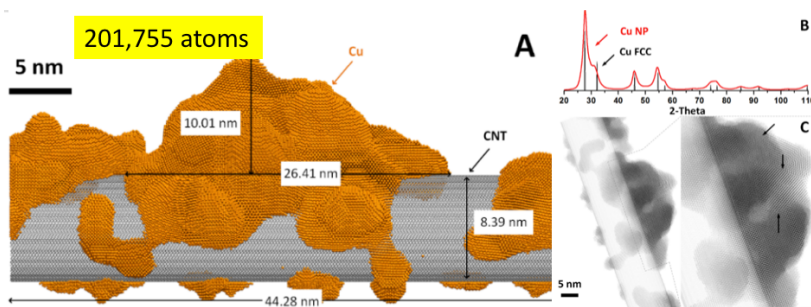


Figure 9. Starting with the structure in Figure 8, we selected 200 surface sites and used QM to calculate the CO binding for an A cluster (~80 atoms). We found 4 that bonded most strongly.

We then calculated the transition state for the key step for producing ethanol and found that 2 of the 4 had low barriers, one of which shown here. [14]

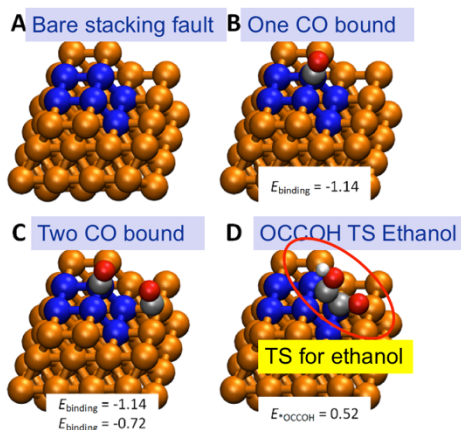


Figure 10. Illustration for the Machine Learned model to predict CO reduction performance on the Cu NP. [15]

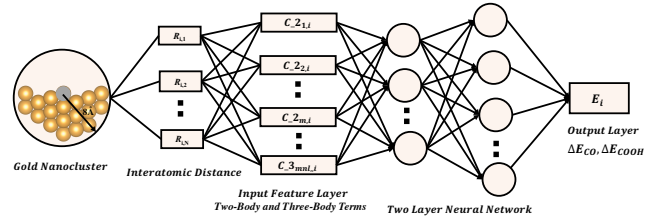


figure 11

Predicted CO binding energy for all 11,000 on the Cu NP from ReaxFF. [15]

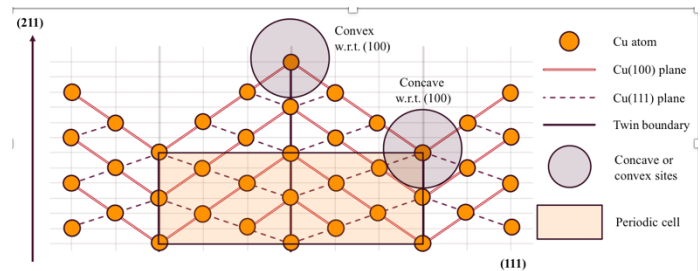
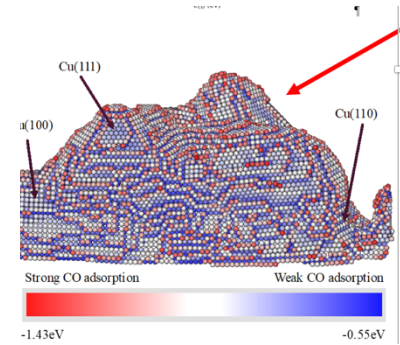


Figure 12. Predicted optimum site for ethanol production on the Cu NP built on a 4x5 until cell. We predict 96% FE for this system.[15]

Figure 13. Reaction mechanism predicted for  $\gamma$ -FeNi-OOH using B3PW91 hybrid DFT theory. The onset potential predicted from the microkinetics is 0.42 V for a current of 10 mA/cm<sup>2</sup> with a Tafel Slope of 24 in reasonable agreement with experiments: 0.37 V f onset potential and a Tafel Slope of 30.[16]

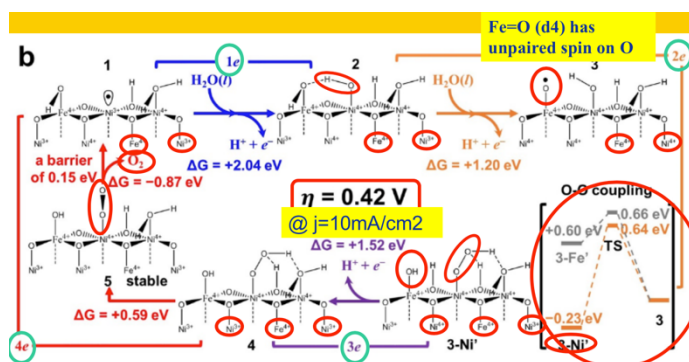


Figure 14. The reaction mechanism and performance for the OER on Sen Zheng's Co/TiO<sub>2</sub> NP. [19]

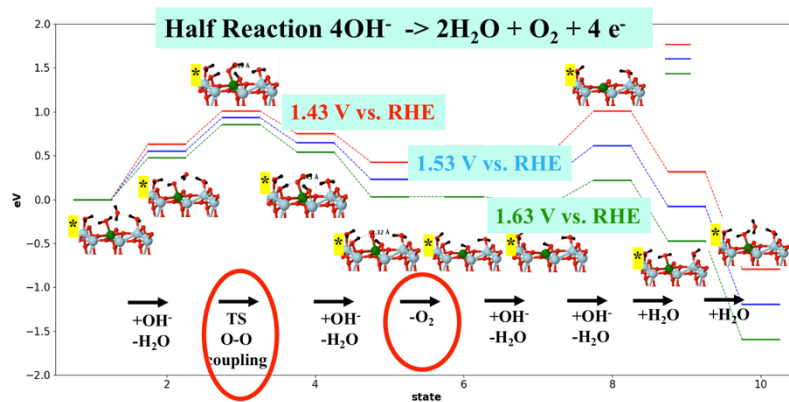
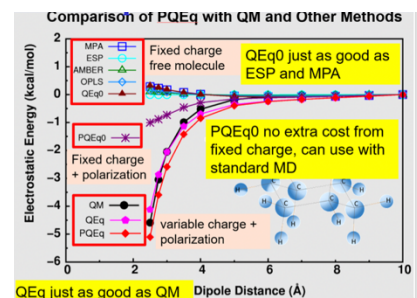


Fig 15. Comparison between QM and the PQEq predicted polarization of cyclohexane as a point dipole is brought up. Standard FF such as Amber cannot account for this. [21]



## Properties water

	Empirical FF					DFT-QM		DFT based FF	
	Expt.	RexPoN	TIP3P	TIP4P-2005	SPC/E	PBE	SCAN	MB-pol	CC-pol
$T_{\text{melt}}$	273.15	273.3	146	252	215	420	-	263.5	-
$S^0$	69.9	68.43	72.51	57.47	60.30	51.32	-	-	-
$\rho$	0.9965	0.9965	0.98	0.993	0.994	0.944	1.050	1.007	-
$\epsilon$	78.4	76.1	94	58	68	112	-	68.4	-
$\Delta H_v$	10.52	10.36	10.05	11.99	11.79	6.20	-	10.93	10.89
$R_1$	2.86	2.84	2.79	2.77	2.75	2.71	2.74	2.81	2.79
$g_{\text{OO}}(R_1)$	2.50	2.34	2.79	3.22	3.05	3.69	3.17	2.76	2.77

Fig 16

Predicted properties of from RexPoN compared to experiment and to QM and other FF. [20]

melting temperature  $T_{\text{melt}}$  (K) at 1 atm pressure.  
Standard molar entropy  $S^0$  (J/mol/K)<sup>27</sup>,  
density  $\rho$  (g/cm<sup>3</sup>),  
static dielectric constant  $\epsilon$ ,  
heat of vaporization  $\Delta H_v$  (kcal/mol),  
 $R_1$  (Å) the position of the first peak of  $g_{\text{OO}}$   
all at T= 298 K, p=1 atm.

RexPoN make NO use of empirical data  
Only high level QM  
But it leads to spectacular agreement with experiment